

1989 NASA/ASEE SUMMER FACULTY FELLOWSHIP PROGRAM

**JOHN F. KENNEDY SPACE CENTER
UNIVERSITY OF CENTRAL FLORIDA**

**MATHEMATICAL MODEL FOR ADAPTIVE CONTROL SYSTEM
OF ASEA ROBOT AT KENNEDY SPACE CENTER**

PREPARED BY:

Dr. Omar Zia

ACADEMIC RANK:

Associate Professor

UNIVERSITY AND DEPARTMENT:

**California Polytechnic State University
Engineering Technology Department**

NASA/KSC

DIVISION:

Mechanical Engineering

BRANCH:

Special Projects (RADL)

NASA COLLEAGUE:

Mr. V. Leon Davis

DATE:

August 23, 1989

CONTRACT NUMBER:

**University of Central Florida
NASA-NGT-60002 Supplement: 2**

ABSTRACT

This paper discusses the dynamic properties and determines the mathematical model for the adaptive control of the robotic system presently under investigation at Robotic Application and Development Laboratory at Kennedy Space Center.

NASA is currently investigating the use of robotic manipulators for mating and demating of fuel lines to the Space Shuttle Vehicle prior to launch. The Robotic system used as a testbed for this purpose is an ASEA IRB-90 industrial robot with adaptive control capabilities. The system was tested and it's performance with respect to stability was improved by using an analogue force controller.

The objective of this research project is to determine the mathematical model of the system operating under force feedback control with varying dynamic internal perturbation in order to provide continuous stable operation under variable load conditions. A series of lumped parameter models are developed. The models include some effects of robot structural dynamics, sensor compliance, and workpiece dynamics.

SUMMARY

The Robot Application and Development Laboratory at Kennedy Space Center has been tasked to address the unique needs of the center in preparing, ground servicing and launching the nation's spacecraft. Unlike industrial applications, these are not monotonous repetition of relatively simple tasks but occasional/intermittent performance of very sophisticated tasks. To achieve the goal, Robotic Application Laboratory has put together a state of the art robotic system which provides an excellent and easy to use testbed. The goal is to provide an experimental testbed to examine possible robotic solutions for a wide variety of tasks which might benefit the center in terms of safety, quality, reliability or cost saving.

Mating and demating of umbilical fuel lines for the main tank of the Space shuttle vehicle is one area that Robotic Application and Development Laboratory is working on. In order for a robot to accomplish the task of umbilical mating the following three distinct phases must occur.

- o Vision tracking must take place to allow the robot to approach and track the umbilical socket.
- o The second phase is the actual mating process to occur which require a combination of mechanical guidance, compliance and active force feedback.
- o The last phase happens when a solid mating has occurred. This is the most critical part of the process where the random motions of the Space Shuttle Vehicle has to be duplicated by the robot using a force feedback approach to avoid large contact forces.

Initial experimental tests had indicated that the existing robotic system had tendency of becoming unstable while following the random motions of the Space Shuttle Vehicle simulator. This problem was investigated thoroughly in the summer of 1988.

The cause of the problem was traced (240 msec time delay in the adaptive control path). An alternate method of implementing force control to provide proof of concept to avoid time delay was developed. The goal in this research project is to determine the mathematical model of the system . The closed loop performance of the system has been observed in the laboratory to be stable and satisfactory for most applications. The particular properties of the system that can lead to instability and limit performance has been discussed. A series of lumped parameter models are developed in an effort to predict the closed loop dynamics of force controlled arm. While experimental tests indicated the computational time delay to be the main source of instability, qualitative analysis shows that the robot dynamics can have significant contribution to the system's instability.

TABLE OF CONTENTS

Section	Title
1.	INTRODUCTION
2.	FORCE CONTROL GENERAL CONSIDERATIONS
2.1	ADAPTIVE CONTROL FEATURE OF RADL SYSTEM
2.2	FORCE CONTROL FEATURE OF RADL SYSTEM
2.3	FORCE CONTROL USING ASEA'S ADAPTIVE APPROACH
3.	DYNAMIC MODELS OF FORCE FEEDBACK ROBOT
3.1	CASE #.1 ROBOT TREATED AS A RIGID BODY
3.1.2	CASE #.2 FLIGHT SIDE DYNAMICS INCLUDED
3.1.3	CASE #.3 ROBOT DYNAMICS INCLUDED
4.	MATHEMATICAL MODELS OF FORCE FEEDBACK CONTROL FOR ASEA
4.1	GENERAL DESCRIPTION OF ASEA ROBOT
4.2	ACCURATE MODEL WITH GENERAL PARAMETERS
4.3	EXPERIMENTAL RESULTS
5.	CONCLUSIONS
6.	REFERENCES

1. INTRODUCTION

Motion of robots can be accurately described by coupled sets of highly nonlinear ordinary differential equations. Closed form analytical solutions for these equations are not easily available. Physically the coupling terms represent gravitational torques, which depend on positions of the joints; reaction torques, due to acceleration of other joints; and of course Coriolis and centrifugal torques. The magnitude of these interaction torques depends on the physical characteristics of the manipulator and the load it carries.

The effects mentioned above complicate the task of accurately determining model of the system. Therefore simple tasks like inserting a peg in the hole as well as complicated ones like following the random motions of flight simulator must be broken down into subtasks. Much work has been done by many researchers on the subject of force control for robotic manipulators [1], [2], [3], [4], [5]. One of the problems confronting anyone trying to assimilate this information is that there seem to be as many different techniques and models for force control as there are researchers in the field. After reviewing many of these results, I have attempted to come up with an approximate model for the system under investigation in Robotic Application and Development Laboratory at Kennedy Space Center.

While my main goal is to discuss force control models it should be noted that a force controller must always be used in conjunction with a position controller. Most commonly one wants to specify force control only along selected cartesian degrees of freedom while the remainder are controlled according to position trajectory.

2. FORCE CONTROL, GENERAL CONSIDERATIONS

In general if we put the issue of coordinate transformation aside for the moment, each axis of a force controlled arm can be viewed as a single input (the motor), dual output (position sensor and force sensor) system. The method by which the signals are processed and feedback to the motor determines the performance characteristics of the servo loop. Although it is impossible to make an unequivocal classification of all force servos, it is possible to group most algorithms into three broad categories: torque based, velocity based or position based. This classification is based upon the concept of successive loop closure, that is, closing an inner loop on one sensor and then closing an outer loop using another sensor.

In general the situation is illustrated in Figure 1, showing the sensor signal being processed along with command input, to form a corrective command for the manipulators motors. This model is appropriated for most electric arms where the basic control variable is motor torque. However, it is possible to have three different situations:

- o The force sensor signal is processed to become a torque command.
- o The force sensor signal is processed to become a velocity command to a inner velocity loop or
- o the force signal is processed to become a position command to a inner position loop .

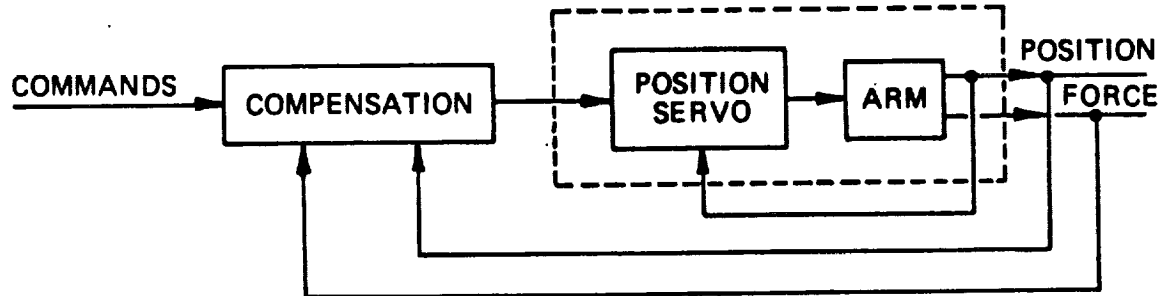


Fig. 1. Generalized force feedback servo with inner position loop

2.1 ADAPTIVE CONTROL FEATURE OF RADL SYSTEM

The problem of self-adjusting the parameters of a controller in order to stabilize the dynamic characteristics of a process, when the plant parameters undergo large and unpredictable variations, has led to the development of adaptive control techniques. Adaptation, in some sense, can be viewed as "combined identification and control of a particular system"

Since adaptive control has very extensive scope , therefore it is necessary to clarify what we have in mind by the term "Adaptive Control".

The role of adaptation mechanism can either be :

- o A parametric adaptation, by adjusting the parameters of the simulated plant, or
- o Signal-synthesis adaptation, by applying an appropriate signal to the input of the plant.

In the case of ASEA Robotics System which is used in the Robotic Application and Development Lab (RADL), the use of "Adaptive Control" implies the ability to adapt to real world changes as determined by sensory devices, by changing the input to the system. Since the sensory device (force/torque sensor) is sensing the force therefore it is also considered as force control.

The original intent of including "Adaptive Control feature on the ASEA robot was to allow external sensors to modify the trajectory of the robot to compensate for the irregularities and uncertainties in welding and gluing operations. Trajectory modifications through the adaptive control inputs allow real time adaptation of the path

2.2 FORCE CONTROL FEATURE OF RADL SYSTEM

AS was mentioned before the goal of RADL is to accomplish the mating of an umbilical fuel line to a moving target representing the external tank of the Space Shuttle Vehicle (SSV). To perform this a vision system is first used to approach and track the target. This is followed by mating the robot-maneuvered umbilical plate to the SSV hardware. While it is mated the hard part of the process must take place namely the robot must duplicate the random motion of SSV to avoid any large contact forces and damage to the SSV. Finally, the force controller must allow the withdrawal of the mating plate and return control back to the vision system.

During contact between the robot and an external object in this case the random motion simulator (RMS) table, forces are generated. Since the system is typically quite stiff, relatively large forces can be created by small motions. The contact force can be modified by commanding small changes in the robot's position to adjust the force to desired value. Typically the desired contact force must be large enough to allow the robot to remain in contact with the object.

One very straightforward approach to force control is called damping Control. With this method the command velocity of the robot is proportional to and in the direction opposite the applied force. In effect, the robot moves so as to relieve the forces generated during elastic contact. this approach makes the robot appear as a viscous damper.

The proportional constant between the commanded velocity and the voltage signal representing the force is called the control gain. this value approximately determines the forces that are seen at a given speed. The proper selection of the controller gain will be a prime goal in the development of the force controller. Typically, the higher the control gain, the lower the apparent damping value of the robot. This results in lower contact force for a given tracking speed. However, the higher the control gain, the more prone a system is to instability.

2.3 FORCE CONTROL USING ASEA's ADAPTIVE APPROACH

The general configuration of RADL robotic system is depicted in Fig.2. This is a functional representation of ASEA controller with force feedback.

ASEA's controller is capable of operating the robot under force control by using the Adaptive Control software package. With this approach, a correction vector is programmed prior to operation of the robot. The velocity along the vector is set proportionally to an external input signal. The analogue output signals of the JR3 are able to work directly with these inputs. The adaptive control port operates in a damping control mode, as the resulting velocity is proportional to the input voltage (force signal).

Force control through the Adaptive Control software has been achieved in the lead-around demonstration. Further, force control when the robot is in contact with a rigid object can be achieved using the Adaptive Control software, provided that the controller gain is set low enough. At this value, the motion of the robot is extremely slow for a given force, and the force/velocity performance is far from the required values.

A significant point involved in the use of the ASEA robot with force feedback control is that only the terminal points can be programmed or downloaded from an external computer. The actual trajectory for the endpoint is generated internally by an interpolation routine, as diagrammed in Fig.2. The ramification of this observation is that only modifications of the trajectory endpoints can be made using an external computer. The real-time trajectory as defined by the interpolation routine, can not be modified by this approach. The importance of this observation is dependent on the relative time scales involved. For the existing vision system, trajectory endpoints can be updated at a rate of between 7 and 10 hz. With a new trajectory determined at each interval and with the robot not being required to finish its initial trajectory the robot's dynamics are slow enough to smooth out these trajectory variations.

However for systems requiring rapid modifications, such as force/torque feedback control, the time delay associated with computer communication link is expected to be slow enough to cause instabilities in the control.

The adaptive control feature of ASEA robotic system provides a path for X, Y, and Z axis. This feature allows for the preprogrammed trajectories to be modified based on external inputs to the controller. The velocity of the generated trajectory can be modified by an analogue or digital input signal, allowing an integral force feedback control loop to be placed around the existing position control loop, as demonstrated in Fig.2

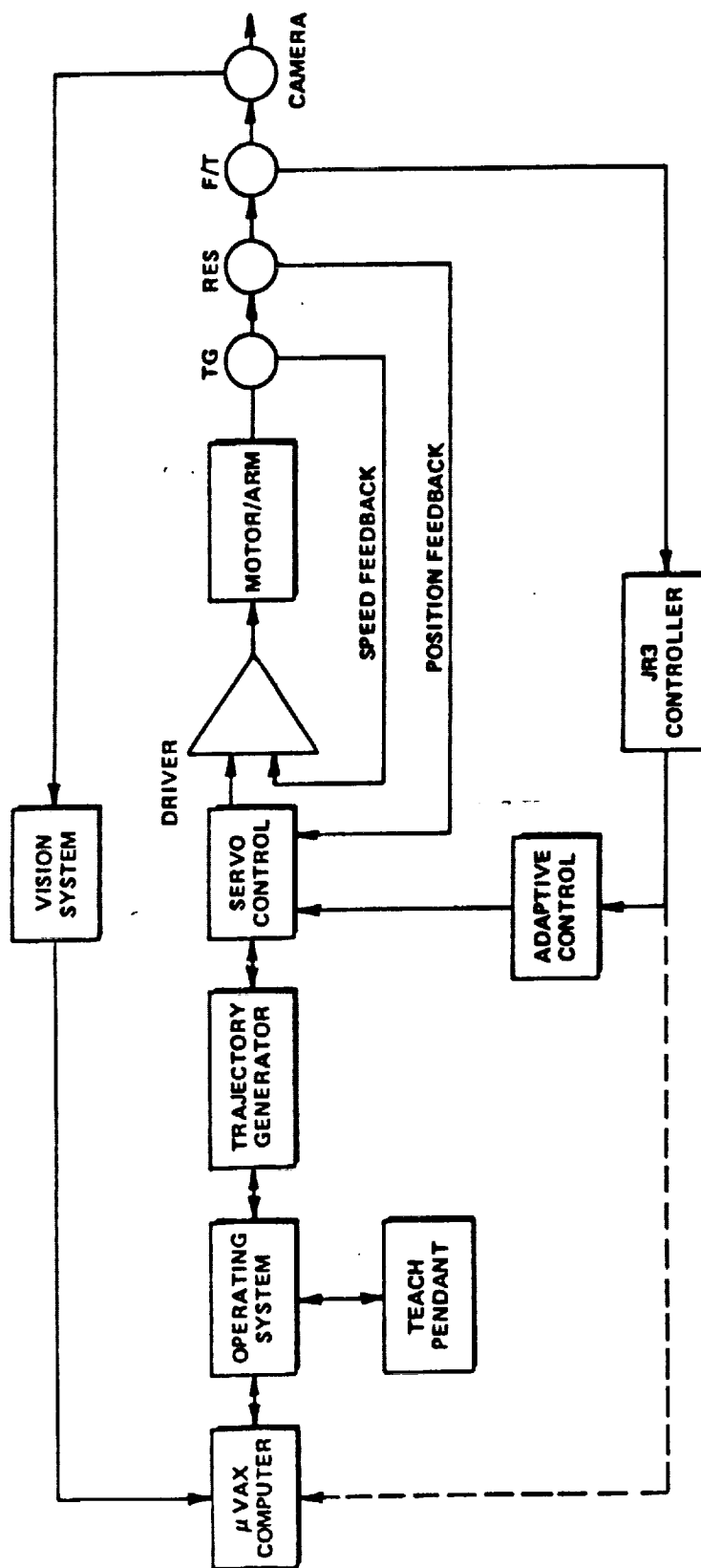


Fig.2: General configuration of RADL robotic control system

3. DYNAMIC MODELS OF FORCE-FEEDBACK ROBOT

3.1. CASE #.1. To begin with a simple case, let us consider the robot to be a rigid body with no vibrational modes. Let us also consider the workpiece (flight side) to be rigid, having no dynamics. The force sensor connects the two with some compliance as shown in Fig.3.

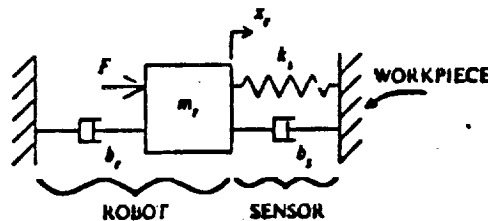


Fig.3: Robot model for case #.1

The robot has been modeled as a mass with a damper to ground. The mass m represents the effective moving mass of the arm. The viscous damper b is chosen to give the appropriate rigid body mode to the unattached robot. The sensor has stiffness k and damping b . The robot actuator is represented by the input force F and the state variable x measures the position of the robot mass.

The open-loop dynamics of this simple system are described by the following transfer function:

$$X(s)/F(s) = 1/[m_r s^2 + (b_r + b_s)s + k_s]$$

Since this robot system is to be controlled to maintain a desired contact force, we must recognize that the closed loop system output variable is the force across the sensor, the contact force F

$$F_c = k_s x_r$$

Implementing the simple proportional force control law :

$$F = k_f (F_d - F_c) \quad k_f \geq 0$$

which states that the actuator force should be some nonnegative force feed-back gain k_f times the difference between some desired contact force F_d and the actual contact force. This control law is embodied in the block diagram of Fig.4.

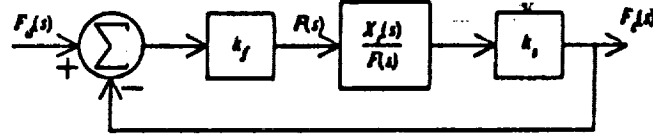


Fig.4 Block diagram for the system of case #.1

The closed loop transfer function then becomes

$$E_c(s)/E_d(s) = k_f * k_s / [m_r s^2 + (b_r + b_s)s + k_s(1 + k_f)]$$

The control loop modifies the the characteristic equation only in the stiffness term. The force control for this case works like a position servo system . This could have been predicted the model in Fig.5 by noting that the contact force depends solely upon the robot position x_r .

For completeness let us look at the root locus plot for this system.

Fig. 5 shows the positions in the s-plane of the roots of the closed loop characteristic equation as the force feedback gain k varies.

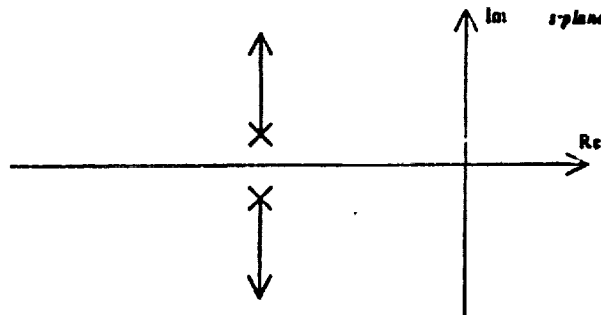


Fig.5 Root locus plot for system of case#.1

C-5

For $k_f = 0$, the roots are at the open loop poles. The loci show that as the gain is increased, the natural frequency increases, and the damping ratio decreases, but the system remains stable. In fact, k_f can be chosen to give the controlled system desirable response characteristic.

3.1.2 CASE #.2 Include flight side dynamics. The simple robot system of Fig.5 has been shown to be unconditionally stable for $k_f \geq 0$. Force controlled systems, however, are not this simple and specially the neglecting of dynamics of the of the environment with which the robot is in contact plays an important role.

Fig.6 is representing the system in which the dynamics of the environment has been taken into consideration. The new state variable is now x_w measures the position .

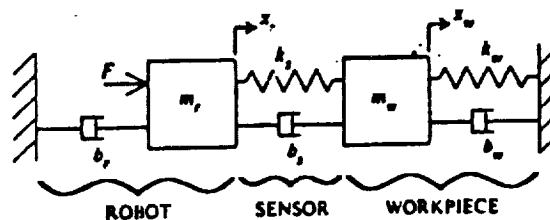


Fig.6: Dynamic model of robot described in case#.2

The open loop transfer function of this two degree of freedom system robot is :

$$X(s)/F(s) = [m_w s^2 + (b_w + b_s)s + (k_w + k_s)]/A$$

$$\text{where } A = [m_r s^2 + (b_r + b_s)s + k_s] * [m_w s^2 + (b_s + b_w)s + (k_s + k_w)] - (b_s s + k_s)^2$$

The output variable is again the contact force F , which is the force across the sensor, given by $F_c = k_s(x_r - x_w)$.

If we now implement the same simple force controller, the control law remains unchanged.

$$F = k_f (F_d - F_c)$$

The block diagram for this control system is shown in Fig.9.

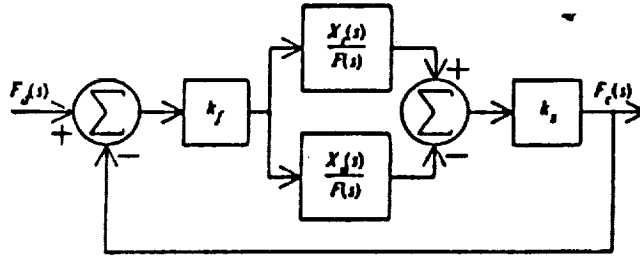


Fig.7 : Block diagram for the system of case #.2

Note that the feedforward path includes the difference between the two open loop transfer functions.

The root locus for this system is plotted in Fig.8 as the force feedback gain k_f is varied.

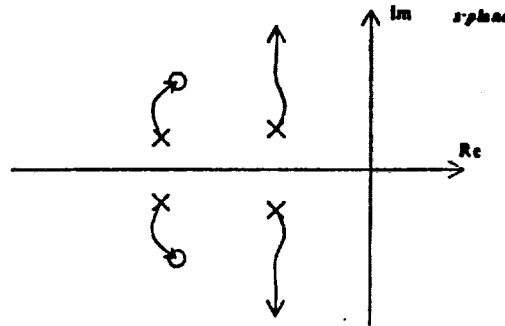


Fig.8 : Root locus plot of system of case #.2

As the root locus indicates there are four open loop poles and two two open loop zeros. The plot then still has two asymptotes at $+90^\circ$. The shape of the root locus plot tells us that even for high values of gain, the system has stable roots. Therefore, while the characteristic of the workpiece affect the dynamics of the robot system, they do not cause unstable behavior.

3.1.3 CASE #.3. INCLUDE ROBOT DYNAMICS

Since the addition of the flight side dynamics to the simple robot system model did not result in the observed instability, we will consider a system with a more complex robot model. If we wish to include both the rigid-body and first vibratory modes of the arm, then the robot alone must be represented by two masses. Fig 9 shows the new system model.

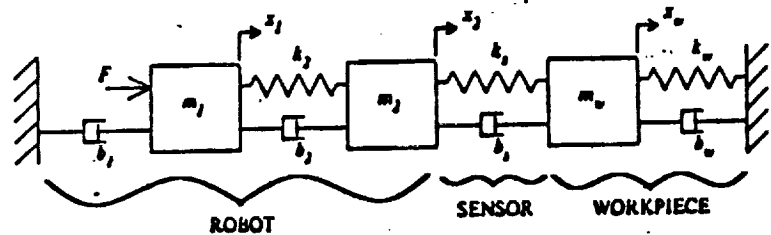


Fig.9 : Robot system model described in case #.3.

The total robot mass is now split between m_1 and m_2 . The spring and the damper with values k_2 and b_2 set the frequency and damping of the robot's first mode, while the damper ground, b_1 , primarily governs the rigid-body mode. The stiffness between the robot mass could be the drive train or transmission stiffness, or it could be the structural stiffness of a link. The masses m_1 and m_2 would then be chosen accordingly. The sensor and workpiece are modeled in the same manner as in case #.1 and case #.2. The three state variables x_1 , x_2 and x_w measure the positions of the masses m_1 , m_2 and m_w .

This-mass model has the following open-loop transfer function:

$$\begin{aligned}
 X_1(s)/F(s) &= A/Y, \quad X_2(s)/F(s) = B/Y \quad \text{and} \quad X_w(s)/F(s) = C/Y \\
 \text{where} \\
 A &= [m_2 s^2 + (b_2 + b_3)s + (k_2 + k_3)] * [m_w s^2 + (b_3 + b_w)s + (k_3 + k_w)] - (b_3 s + k_3)^2 \\
 B &= [m_w s^2 + (b_3 + b_w)s + (k_3 + k_w)] [b_2 s + k_2] \\
 C &= [b_2 s + k_2] [b_3 s + k_3] \\
 Y &= [m_1 s^2 + (b_1 + b_2)s + k_2] * [m_2 s^2 + (b_2 + b_3)s + (k_2 + k_3)] * [m_w s^2 + (b_3 + b_w)s + (k_3 + k_w)] - \\
 &\quad - [m_w s^2 + (b_3 + b_w)s + (k_3 + k_w)] [b_2 s + k_2] - [m_1 s^2 + (b_1 + b_2)s + k_2] [b_3 s + k_3]^2
 \end{aligned}$$

The contact force is again the force across k ,

$F_c = k_s(x_2 - x_w)$
and the simple force control law is

$$F = k_f(F_d - F_c) \quad (k \geq 0)$$

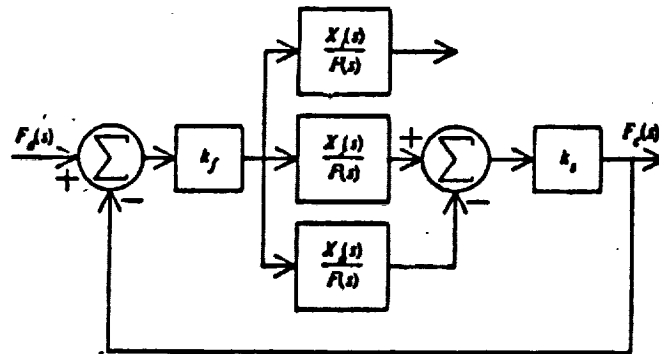


Fig.10: Block diagram of the system of case #.3

The block diagram for this controller, Fig.10, shows again that the feedforward path takes the difference between two open-loop transfer functions

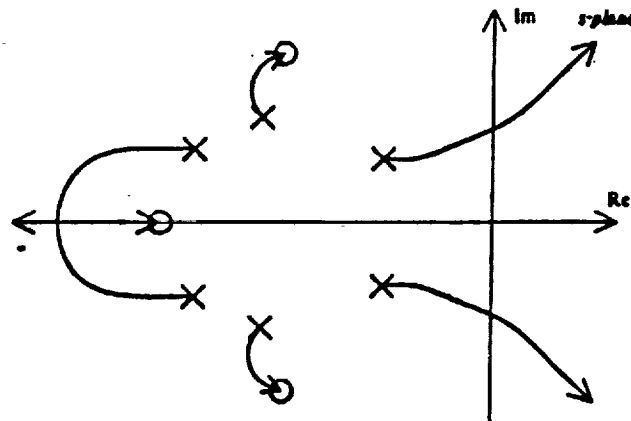


Fig.11: Root locus plot for the system of Fig.12

The root locus plot, Fig.11, shows a very interesting effect.

The system is only conditionally stable.

For low values of k , the system is stable; for high values of k , the system is unstable; and for some critical value of the force feedback gain, the system is only marginally stable.

The + 60 asymptotes result from the system's having six open loop poles, but only three open loop zeros. Inspection of the open-loop transfer function confirms this: the numerator of the transfer function relating $X(s)$ to $F(s)$ is a third-order polynomial in s .

4. MATHEMATICAL MODEL OF FORCE FEEDBACK CONTROL , FOR (ASEA) ROBOT

4. 1 GENERAL DESCRIPTION OF ASEA ROBOT

The ASEA IRB 90 robot is a six axis manipulator coupled with a sophisticated controller. While fig. 2 provided functional representation of the ASEA robot , fig. 12 represents the control system for each axis of the robot.

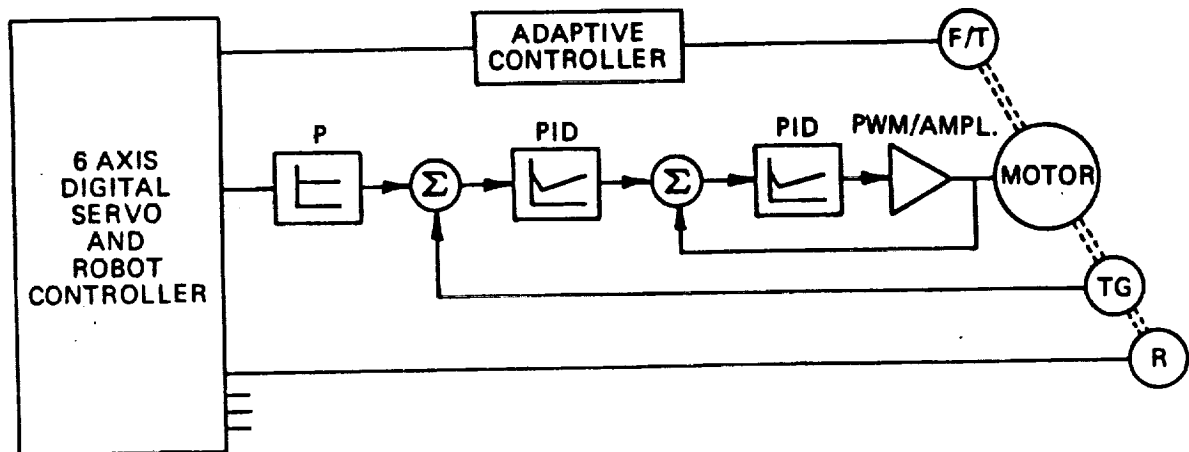


Fig.12 Block diagram of control system for each axis of the robot.

Each robot joint is driven by a DC motor through a redactor. The motors are powered by Pulse Width Modulation circuits using armature voltage control technique. The controller uses both velocity and position feedback signals in a conventional manner, with the PID inner velocity feedback loop surrounded by a position control loop. In order to limit the armature current and to improve the linearity of the system a current feedback loop is also employed.

4.2 ACCURATE MODEL WITH GENERAL PARAMETERS

Based on the block diagram depicted above and the operation of the random motion simulator, it is clear that case #. 2 described in section 3 of this paper is most appropriate to be used as base model.

Using the force dependent voltage from the force/ torque sensor allows the ASEA's adaptive control software to generate a change in the velocity based on an error between the observed force and a bias value representing the force setpoint value.

Fig. 15 is block diagram representation of model of force feedback control structure. The equations governing the system is as following.

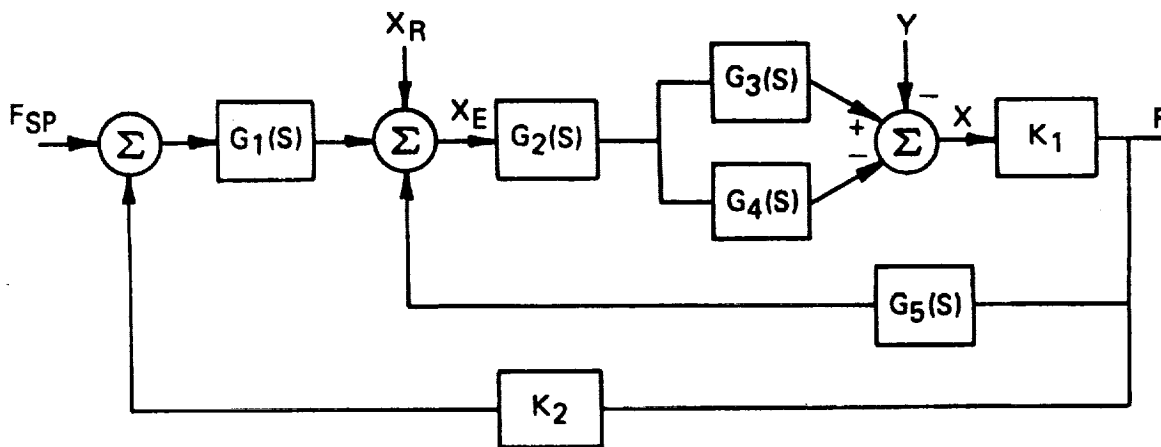


Fig. 13. Block diagram representing model of force feedback control

$$X_e = X_R + G_1(S)(F_{SET} - K_2 F) - G_5(S)F$$

$$X_e = X / \{ [G_2(S)] [G_3(S) - G_4(S)] \}$$

$$X_R + G_1(S)(F_{SET} - K_2 F) - G_5(S)F = X / \{ [G_2(S)] [G_3(S) - G_4(S)] \}$$

This would be the model that governs the behavior of the robot when operating in a lead around mode, because of the lack of coupling between the motion of the SSV and the generated force. When in contact with a rigid body the interaction between the robot and an external motion becomes coupled and is modeled as a stiff elastic member.

$$F = K(X - Y) \quad , \quad X = F/K + KY$$

$$[F/K + KY]/\{[G_2(S)][G_3(S) - G_4(S)]\} = X_R + G_1(S)(F_{SET} - K_2 F) - G_5(S)F$$

$$[G_2(S)][G_3(S) - G_4(S)] = G_X(S)$$

$$[F/K + KY]/G_X(S) = X_R + G_1(S)(F_{SET} - K_2 F) - G_5(S)F$$

$$[F/K + KY] = X_R G_X(S) + G_X(S) G_1(S) F_{SET} - G_X(S) G_1(S) K_2 F - G_X(S) G_5(S) F$$

$$F/K = X_R (G_X(S)) + G_X(S) G_1(S) F_{SET} - G_X(S) G_1(S) K_2 F - G_X(S) G_5(S) F$$

$$F[1/K + G_X(S) G_1(S) K_2 + G_X(S) G_5(S)] = X_R G_X(S) + G_X(S) G_1(S) F_{SET}$$

$$F = [X_R G_X(S) + G_X(S) G_1(S) F_{SET}] / [1/K + G_X(S) G_1(S) K_2 + G_X(S) G_5(S)]$$

To make the model practical, it is needed to determine the transfer functions of each block .

1. $G_2(S) = G_m(S) * G_c(S)$, where $G_m(S)$ is the well known transfer function for the torque output vs applied voltage for a DC motor is given :

$$G_m(S) = \frac{K_t}{K_t K_e + RB} * \frac{JS + B}{JL/[K_t K_e + RB] S^2 + [JR + LB]/[K_t K_e + RB] S + 1}$$

2. $G(S)$ is the transfer function of the compensator = $K_p + K_I/S$

3. $G(S)$ is the transfer function of the adaptive control path which was determined [3] to be equal to K/S without delay and $K/S * e^{-Ts}$ with delay.

4. $G_3(S) = X_r(S)/F(S)$, $G_4(S) = X_h(S)/F(S)$, related to robot and flight simulator dynamics and were determined in section 3.

The model is still theoretical until the coefficients of the transfer function are determined. In order to obtain concrete parameters of the system, one can use two different methods. Using catalogues and manufacturer's data or direct measurement. While manufacturer's data can often be accurate, accuracy of direct measurement obviously depends on precision in measurement. In our case unfortunately obtaining data from manufacturer was not possible, so the only alternative was to rely on direct measurement of frequency and time response of the system, which led to a simple single degree-of-freedom model as shown in Fig.14.

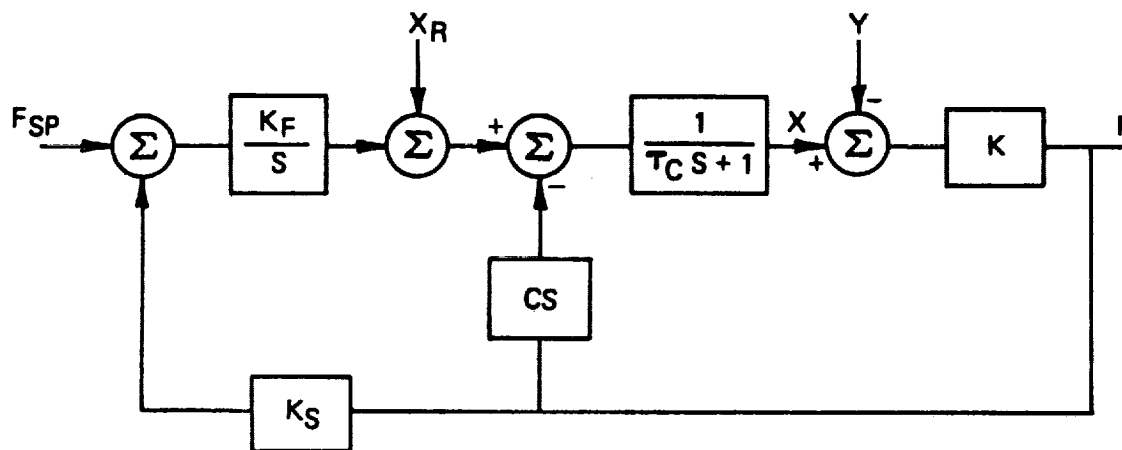


Fig. 14 Approximate model of the system

4.4 EXPERIMENTAL RESULTS

Fig. 15 is the time response of the system, figures 16 and 17 represent the frequency response of the system. Fig 18 demonstrates a significant time lag that exists in the adaptive control software for force control. It was determined by simultaneously plotting the reference voltage into the adaptive control port and the resulting motion. This delay also could be identified via frequency response analysis. Fig. 18 demonstrates the tremendous phase lag encountered at higher frequencies, as typically found in systems with a time delay. An approximate transfer function has been determined by [3] which provides a fairly good fit.

$$X(S)/V(S) = \frac{6.0 e^{-.3S}}{S(0.1429 S + 1)}$$

From this transfer function and the data obtained by [3], the following values may be assigned: $T = 0.1429$, $K_f = 6$, $K = 134 \text{ lb/in}$, $K_s = 0.004 \text{ V/lb}$.

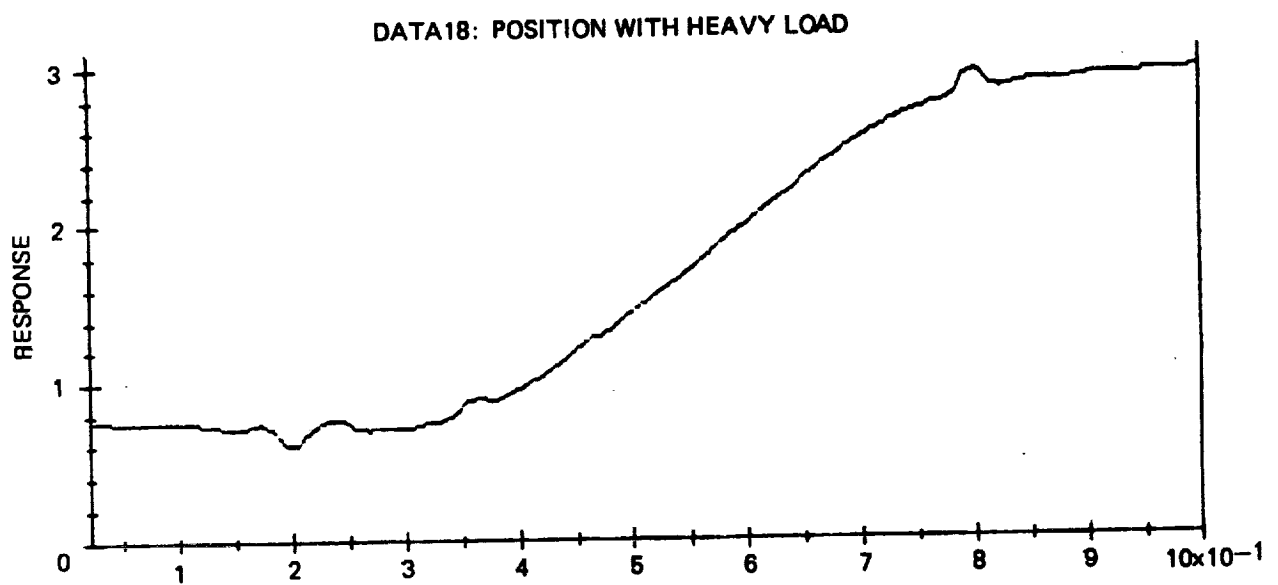
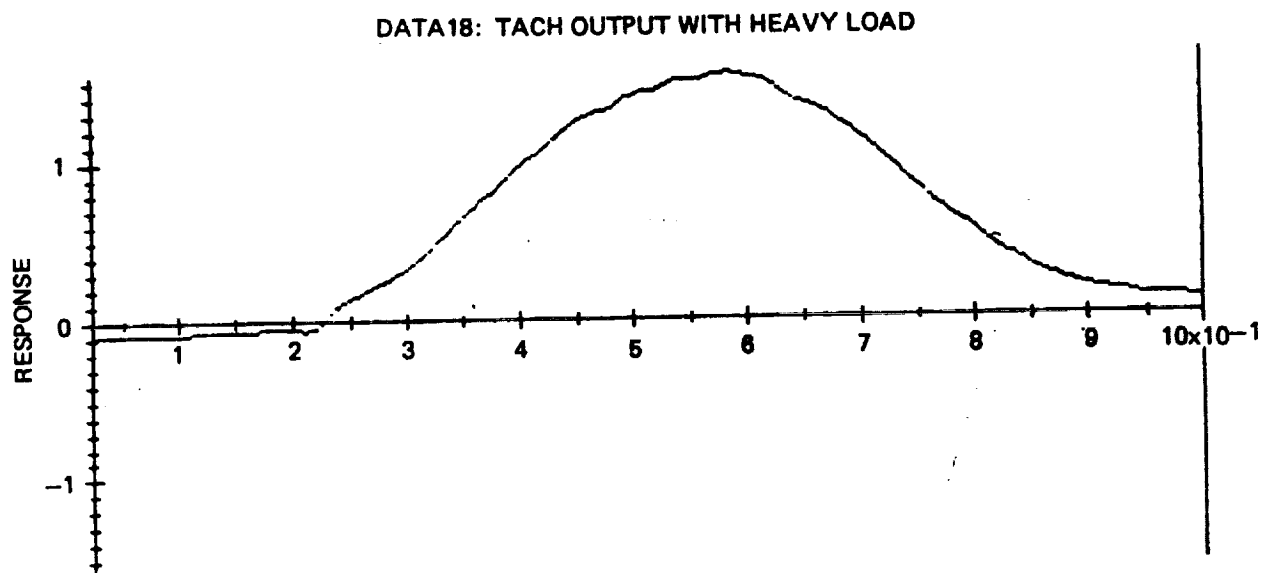


Fig. 15 Time response

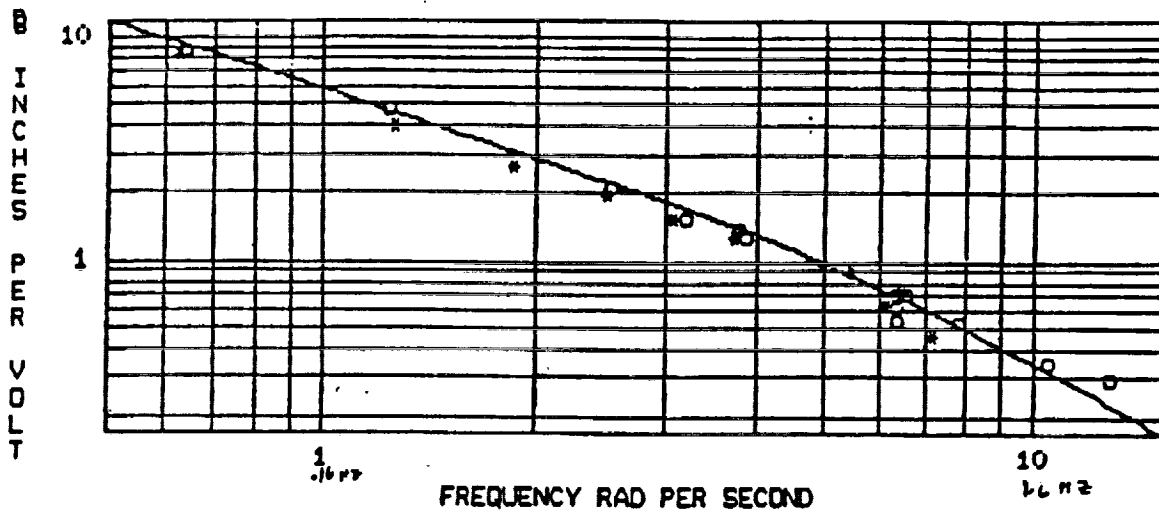


Fig. 16 Frequency response plot of base rotation axis

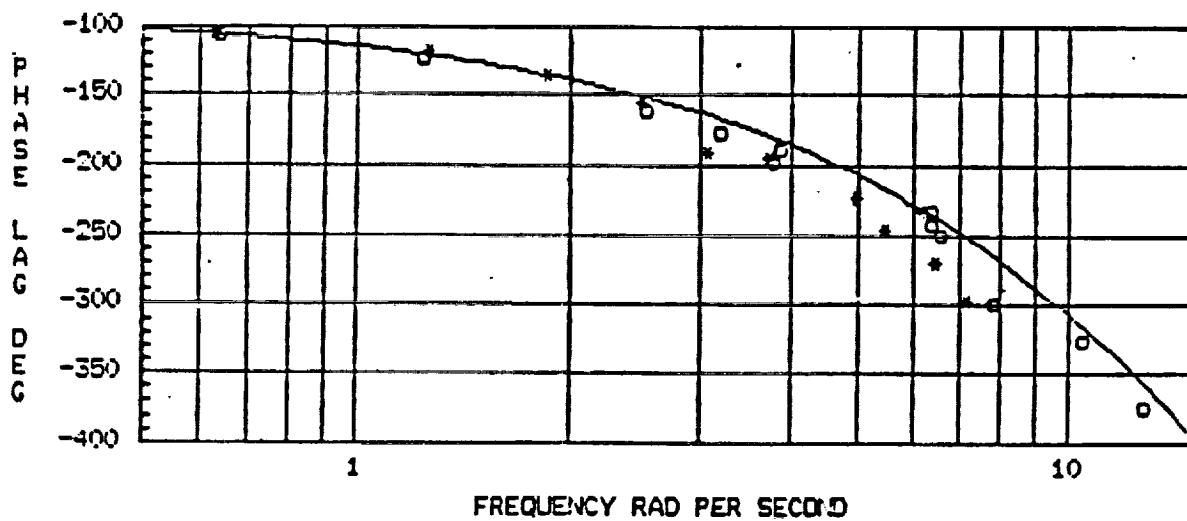
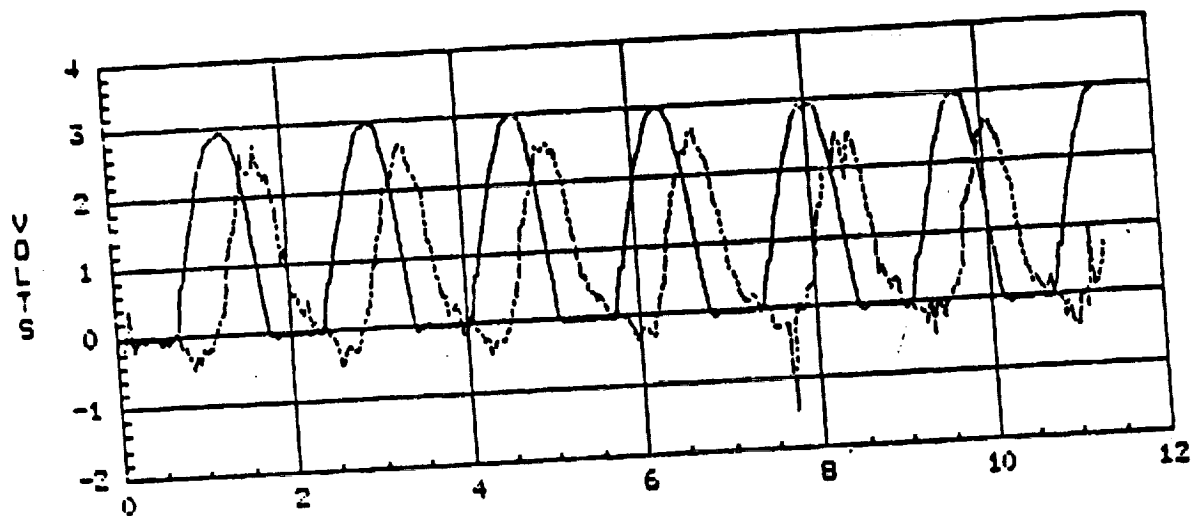


Fig. 17 Frequency response plot of base rotation axis



Delay in ASEA controller between
input voltage and resulting
servo command voltage

5. CONCLUSIONS

An accurate lumped parameter model for the control system of ASEA robot has been developed. Efforts to determine concrete values for the parameters has been unsuccessful. However, an approximate linear model with concrete parameters to replace the accurate model has been suggested.

Although no theoretical proof has been presented, practically it was found out that time delay between the output and input signals in ASEA controller can cause instability. Without the controller latency, stable force control during both tracking and mating can be achieved. The combination of passive compliance and force control provide excellent performance when mated.

More over a series of lumped- parameter models has been developed in order to understand the effects of robot and workpiece dynamics on the stability of simple force controlled systems. An instability has been shown to exist for robot models that include representation of a first resonant mode for the arm. The effect of the workpiece dynamics remains unclear. It has been shown that when the workpiece is modeled as a rigid wall, the system can be unstable. Certainly if the workpiece were very complaint and extremely light there could be no force across the sensor, degenerating the closed loop system to the open loop case, which ofcourse is stable. The sensor and workpiece dynamics are therefore important and should be modeled. Limited actuator bandwidth, filtering, and digital controller implementation can also cause instability. These performance limitations must also be included in the system model used for controller design.

6. REFERENCES

- [1] S. D. Eppinger and W. P. Seering, "On Dynamic Models of Robot Force Control,"
Proc. Int. Conf. Robot. Autom., April 1986.
- [2] O. Zia, "Adaptive Servo Control for Umbilical Mating."
1988 NASA/ASEE Summer Faculty Report, University of Central Florida.
- [3] R. Rees Fulmer, "The Development of Force Feedback Control for Umbilical Mating,"
Final Contract Report, RADL, Kennedy Space Center Florida.
- [4] D. E. Whitney, "Force Control of Manipulator Fine Motions,"
J. Dyn. Syst., Measurement and Control, Vol.99, June 1987.
- [5] E. Carrizosa, V. Feliu, "Study of the Dynamical Behavior of an Assembly Robot,"
Robot Control (SYROCO'85), Proc. of 1st IFAC Symposium, Spain, Nov. 1985.
- [6] E. M. Onaga and L. L. Woodland, "Six-axis Digital Torque Servo"
Proc. Int. Symposium on Industrial Robot, April 1987.